

# Influences of forested and grassland vegetation on late Quaternary ecosystem development as recorded in lacustrine sediments

Kendra K. McLauchlan<sup>a,\*</sup> , Ioan Lascu<sup>b,c,\*</sup> , Emily Mellicant<sup>a</sup>, Robert J. Scharping<sup>a,d</sup> , Joseph J. Williams<sup>e</sup> 

<sup>a</sup>Department of Geography, Kansas State University, Manhattan, Kansas 66506, USA

<sup>b</sup>Department of Mineral Sciences, National Museum of Natural History, Smithsonian Institution, Washington, DC 20560, USA

<sup>c</sup>Department of Earth Sciences, University of Cambridge, Downing Street, Cambridge, CB2 3EQ, United Kingdom

<sup>d</sup>Department of Cell Biology, Microbiology and Molecular Biology, University of South Florida, Tampa, Florida, USA

<sup>e</sup>Department of Geography, Oxford Brookes University, Oxford, United Kingdom

\*Corresponding author e-mail address: [mclauch@ksu.edu](mailto:mclauch@ksu.edu) (K.K. McLauchlan), [lascui@si.edu](mailto:lascui@si.edu) (I. Lascu).

(RECEIVED June 10, 2018; ACCEPTED November 26, 2018)

## Abstract

Geosphere-biosphere interactions are ubiquitous features of the Earth surface, yet the development of interactions between newly exposed lithologic surfaces and colonizing plants during primary succession after glaciation are lacking temporal detail. To assess the nature, rate, and magnitude of vegetation influence on parent material and sediment delivery, we analyzed ecosystem and geochemical proxies from lacustrine sediment cores at a grassland site and a forested site in the northern United States. Over time, terrigenous inputs declined at both sites, with increasing amounts of organic inputs toward present. The similarities between sites were striking given that the grassland sequence began in the Early Holocene, and the forested sequence began after the last glacial maximum. Multiple mechanisms of chemical weathering, hydrologic transport, and changes in source material potentially contribute to this pattern. Although there were strong links between vegetation composition and nitrogen cycling at each site, it appears that changes in forest type, or from oak woodland to grassland, did not exert a large influence on elemental (K, Ti, Si, Ca, Fe, Mn, and S) abundance in the sedimentary sequences. Rather, other factors in the catchment-lake system determined the temporal sequence of elemental abundance.

**Keywords:** Holocene; Paleolimnology; North America; Sedimentology; Lakes; Inorganic geochemistry; Vegetation dynamics; Weathering

## INTRODUCTION

One of the fundamental relationships within Earth systems is the interaction between the geosphere and the biosphere. The role of terrestrial plants in shaping newly formed landscapes (i.e., primary succession) has been studied after glacial retreat (Buma et al., 2017), volcanic eruptions (Cutler et al., 2008), and mass movement (Colombaroli and Gavin, 2010). Most Earth surfaces are considered to undergo relatively slow rock weathering processes. These processes are dominated by climatic factors, but vegetation also influences weathering (Pawlik et al., 2016) and vice versa (Hahm et al., 2014). The nature of the geosphere-biosphere relationship, and its spatial and temporal regulators, vary across various climatic, geomorphic, tectonic, and biotic settings (Porder, 2014). Here,

we focus on the biotic setting, comparing the pace and nature of ecosystem development between two major vegetation types—forest and grassland—to improve our understanding of the relative effect of biota on the geochemical composition of sediments over millennial timescales (Jenny, 1941).

To understand landscape development over time, we are often limited to comparing Earth surface features to source rock material. While this can give some indication of how plants may have interacted with rock on timescales of  $10^5$  or  $10^6$  yr, the intermediate steps, rates, and controls of geosphere-biosphere processes are unknown using this approach. Nonetheless, chronosequence studies of primary succession have demonstrated, broadly, how ecosystems change over time. As primary successional stages develop, there is generally a temporal sequence of biogeochemical changes such as base cation mineral weathering, organic matter accumulation from the terrestrial biosphere, increases in plant-available nitrogen, and decreases in phosphorus (Laliberte et al., 2012; Wardle et al., 2004). However, characterizations of these early stages lack high temporal detail. In

**Cite this article:** McLauchlan, K. K., Lascu, I., Mellicant, E., Scharping, R. J., Williams, J. J. 2019. Influences of forested and grassland vegetation on late Quaternary ecosystem development as recorded in lacustrine sediments. *Quaternary Research* 92, 201–215.

particular, we may be missing important system behavior such as tipping points and pedogenic thresholds (Vitousek and Chadwick, 2013).

Early postglacial successional processes can be reconstructed by studying geochemical records of rock-plant interactions in continuously deposited lacustrine sedimentary records (Mackereth, 1966; Pennington et al., 1972; Engstrom and Hansen, 1985). These records provide information on a finer scale (<17,000 yr BP) than is possible in temperate chronosequences. Measuring elemental concentrations in sedimentary sequences has a long history (Likens, 1985; Willis et al., 1997) but, because of the proxy nature of these records, interpretation is aided by a multitude of other parameters describing the properties of these systems (Kylander et al., 2011). Of particular importance are proxies of transport processes from the catchment to the sediment. These dynamic processes are a function of climatic changes, lithological variability, and differences in vegetation cover between grassland and forested catchments. Through multi-proxy investigation, sedimentary sequences have begun to yield unique information about early ecosystem processes. For example, important information about P cycling can be obtained from studying the chemical weathering of the phosphate mineral apatite early in catchment development (Boyle, 2007; Norton et al., 2011).

There are several potential mechanisms for how terrestrial vegetation could determine trajectories of biogeochemical change on centennial to millennial timescales, as seen in Holocene sedimentary records. First, vegetation composition can influence chemical weathering rates. There are examples of organic acids produced by coniferous vegetation speeding ecosystem acidification (Ford, 1990) and even leading to podsolization during the Holocene (Davis et al., 2006). Conversely, removal of trees has been demonstrated to cause an increase in soil pH (Bradshaw et al., 2005). Second, the degree of vegetation cover (primary productivity) can affect hydrologic pathways and physical weathering. Large-scale changes from grassland to forests between stadials and interstadials during the last glacial, with different rates of productivity, led to differences in weathering product delivery to a depositional basin (Kylander et al., 2011). Finally, there are also potential feedbacks between fire regimes and geochemistry. In lodgepole pine forests of the western United States, loss of nitrogen and base cations has occurred over the past 4000 yr with repeated fire (Dunnette et al., 2014; Leys, 2016). While fire events and plant cover were significantly related at Thyl Lake in the French Alps, soil processes were primarily linked to vegetation composition and secondarily to changes in fire regime (Mourier et al., 2010).

To assess rates, patterns, and mechanisms of ecosystem development after glacial retreat, we compared two sedimentary sequences in the upper Midwestern United States from a grassland site and a forested site. Our three main questions were: (1) How did source material change over the sedimentary sequences? (2) What were the patterns of nutrients, especially limiting nutrients such as nitrogen, potassium, calcium, and magnesium, during Holocene ecosystem development?

(3) Did the terrestrial biosphere determine the trajectory of elemental change at each site?

## METHODS

### Study sites

Fox Lake is located in southern Minnesota, USA, has a surface area of 3.85 km<sup>2</sup>, and a maximum water depth of 6 m. The lake was formed during the retreat of the Des Moines Lobe of the Laurentide Ice Sheet at the end of the last glaciation about 12,000 yr (Maher, 1982; Lusardi et al., 2011). Fox Lake is approximately 10 km from the southernmost extent of the Des Moines Lobe, but the timing and path of deglaciation are not entirely clear in this region. The catchment parent material is calcareous glacial till, and lake water geochemistry is dominated by catchment input rather than precipitation-evaporation dynamics (Gorham et al., 1983). There is one small inlet stream on the west side of the lake. Soils surrounding Fox Lake are a mix of Udols and Aquolls—poor to well-drained clay loams formed from calcareous tills—and are often deep (>2m; USDA NRCS, 2018).

Devils Lake is located in southern Wisconsin, has a surface area of 1.53 km<sup>2</sup>, and a maximum depth of 14 m. Catchment parent material is primarily hematite-rich quartzite, as well as glacial till deposited in moraines from the Green Bay Lobe at the end of the last glacial period, ca. 18,500 cal yr BP (Attig et al., 2011). Soils in this area are thin (0.5–1 m) Udalfs—moderately well-drained stony and cobbly silt loams formed from a mixture of loess and quartzite bedrock (USDA NRCS, 2018). Devils Lake is located just to the south of the maximum extent of the Laurentide Ice Sheet. The catchment of Devils Lake has areas of quartzite cliffs and the geology is considerably different than Fox Lake and therefore these two sites capture a wide range of weathering products to lakes.

The two study sites are ~480 km apart (Fig. 1). The sites were chosen due to their positions relative to the furthest advance of the Laurentide Ice Sheet and dominant vegetation cover during the Holocene. At the time of Euro-American settlement (mid-1800s), Fox Lake was tallgrass prairie characterized by warm-season grass species such as *Andropogon gerardii*, *Sorghastrum nutans*, and *Schizachyrium scoparium* (Küchler, 1964). Today, the Fox Lake catchment is dominated by agriculture. In contrast, Devils Lake is surrounded by mixed deciduous-coniferous forest including the conifer *Pinus strobus*, deciduous components of *Quercus rubra*, *Quercus alba*, and *Acer rubrum*, and herbaceous savanna understory vegetation. Modern vegetation between the two sites likely varies due to differences in precipitation. Devils Lake on average receives 914–940 mm of annual precipitation, while Fox Lake receives 762–812 mm of annual precipitation (NOAA, 2018).

In February 2012, we obtained sediment cores from both Devils Lake and Fox Lake using piston corers. The Fox Lake sediment core was 9.3 m long and the Devils Lake sediment core was 10.4 m long.

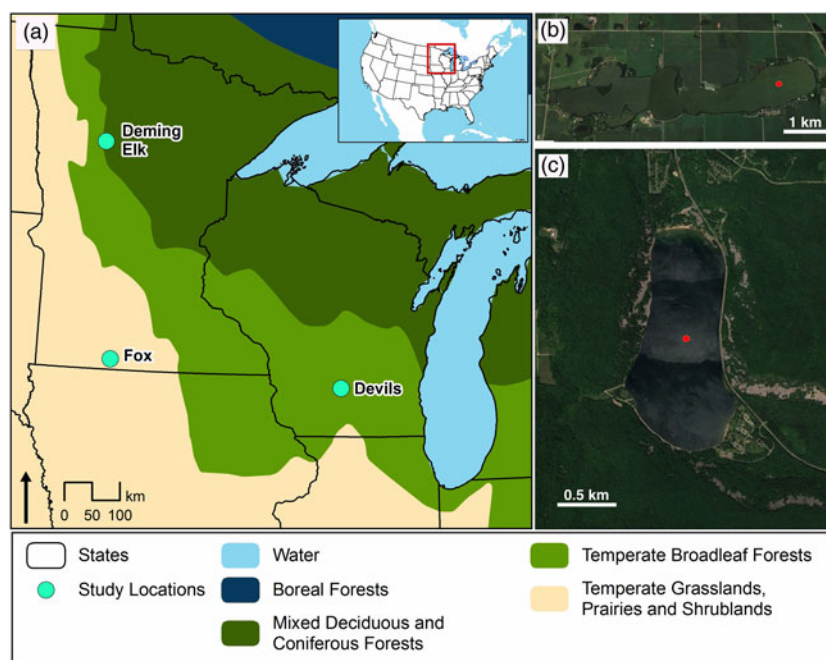


**Figure 1.** (a) Regional map with locations of Fox Lake, Devils Lake, and the other sites referred to in text (Deming Lake AND Elk Lake). (b) Detail of Fox Lake basin morphology and vegetation. (c) Detail of Devils Lake basin morphology and vegetation. Red dots represent coring sites. (For interpretation of the references to color in this figure legend, the reader is referred to the web version of this article.)

A previous study of Fox Lake established a radiocarbon-based chronology as well as the vegetation and fire history (Commerford et al., 2016). The same sediment cores were used to measure the proxies described in the current manuscript. Previously, vegetation history reconstructed by pollen analysis from 9300 cal yr BP indicates that Fox Lake has been a grassland site since near the beginning of the record, with only one slight change from oak forest to grassland at 8200 cal yr BP (Commerford et al., 2016). The oak forest vegetation is characterized by high amounts of *Quercus* pollen (an arboreal pollen type), and the grassland vegetation is characterized by high amounts of non-arboreal pollen types such as *Poaceae*, *Ambrosia*, and *Artemisia*. Thus, for this study we used the % arboreal pollen to capture this vegetation transition at Fox Lake. The lithostratigraphy for Fox Lake is consistently characterized by dark brown, high organic matter sediment throughout the core. Five zones (F1–F5) were determined with constrained hierarchical cluster analysis using changes in magnetic susceptibility (Commerford et al., 2016).

Details of the lithology, radiocarbon chronology, fire history, and geochemical proxy records of Devils Lake are also described previously (Williams et al., 2015). The same sediment cores were used to measure the proxies described in the current manuscript. Devils Lake has a much longer record than Fox Lake, beginning at 17,000 cal yr BP (Williams et al., 2015), and captures three types of forest: spruce, pine, and hardwood (Maher, 1982). The detailed pollen stratigraphy with three forest types was established by Maher (1982) and Williams et al. (2015) established a robust chronology with input from Grimm et al. (2009). The changes

in vegetation from coniferous to hardwood forest types are characterized by changes in spruce pollen (*Picea*), pollen from hardwood trees (*Quercus* and *Ulmus*), and grass pollen (*Poaceae*). The lithostratigraphy of Devils Lake varies throughout the core, with five main zones. Five zones (D1–D5) were delineated based on sediment appearance, composition, and mineralogy (Williams et al., 2015).

The two study sites differ in multiple ways—they cover different time periods (one starting in the late glacial and the other in the Early Holocene), are situated in different geologic terrains, and were analyzed for a different suite of sedimentary proxies—but chiefly provide an important contrast in dominant vegetation type and the degree of vegetation change during their respective records. To put the lithologic, pollen, and sedimentological changes for each lake in context, we use the stratigraphic zones previously delineated and published for each lake (Fox Lake in Commerford et al. [2016] and Devils Lake in Williams et al. [2015]). The same sediment cores were used to establish the stratigraphic zones and also for the new analyses presented in this manuscript for both Fox Lake and Devils Lake (Table 1).

### Micro X-ray fluorescence ( $\mu$ -XRF) core scanning

All sections of the Devils Lake and Fox Lake sediment cores were scanned using an Itrax XRF core scanner (Cox Analytical Systems, Gothenburg, Sweden) at the LacCore X-ray Fluorescence Laboratory housed at the University of Minnesota Duluth Large Lakes Observatory. This instrument produces an optical RGB digital image, a microradiographic digital image, and count data for most elements from

**Table 1.** Proxy variables for various ecosystem processes, measured on sediment cores from the grassland and forested lakes and presented in this manuscript. Original sources for some of the proxy variables shown in this manuscript are also reported here.

Proxy variable	Fox Lake (grassland site)	Devils Lake (forested site)
Charcoal concentrations	Commerford et al. 2016	Williams et al., 2015
Pollen concentrations	Commerford et al. 2016	Maher, 1982
Elemental concentrations (XRF)	This manuscript	This manuscript
% C, % N, $\delta^{13}\text{C}$ , $\delta^{15}\text{N}$	This manuscript	Williams et al., 2015
Magnetic parameters to estimate particle size	–	This manuscript
Laser-based particle size analysis	This manuscript	–

aluminum (atomic number 13) to uranium (92). XRF scans were performed using a molybdenum tube set at 30 kV and 25 mA with a dwell time of 60 s and a step size of 10  $\mu\text{m}$ . The Fox Lake data were reduced by averaging to 1 cm, while the Devils Lake data were averaged to 0.1 cm and then smoothed using a 10-point running mean. The raw count data is expressed as counts/second (cps).

For elements with sufficient counts, we divided the elemental counts by molybdenum coherence (MoCoh) values for each measured interval to account for variation among analytical time periods in the characteristics of the Mo tube. A centered-log ratio (clr) transformation was then performed on the MoCoh-corrected  $\mu\text{-XRF}$  intensities, such that  $I_{\text{clr}} = \ln(I/G)$ , where  $I$  is the intensity of the element transformed, and  $G$  is geometric mean of all the elements analyzed at the same measuring point. We analyzed a set of selected elements that had sufficient counts, and that are important in ecosystem and weathering processes. Although the investigated elements are found in various compounds in the sediment, they can indicate three types of processes: allochthonous, biogenic, and authigenic (Lopez et al., 2006). We used  $\text{Ti}_{\text{clr}}$  and  $\text{K}_{\text{clr}}$  as indicative of detrital input;  $\text{Si}_{\text{clr}}$  and  $\text{Ca}_{\text{clr}}$  as indicative of detrital input, as well as biogenic silica and calcite formation, respectively; and  $\text{Fe}_{\text{clr}}$ ,  $\text{Mn}_{\text{clr}}$ , and  $\text{S}_{\text{clr}}$  as indicative in part of detrital input, as well as redox processes.

To better trace these additional processes, MoCoh standardized values were then divided by Ti counts to obtain a measure of silicate weathering ( $\text{K/Ti}$ ), biogenic silica ( $\text{Si/Ti}$ ), and authigenic mineral precipitation ( $\text{Ca/Ti}$ ,  $\text{Fe/Ti}$ ,  $\text{Mn/Ti}$ , and  $\text{S/Ti}$ ). While none of these elements should be interpreted as uniformly indicating a single process, their variability as assemblages may lead to an improved understanding of lake sedimentation (Martin-Puertas et al., 2017). In conjunction with other proxies, elemental assemblages can be used to assess catchment inputs (both lithological and organic), redox conditions, and potentially aquatic primary productivity.

Elemental concentrations are sometimes non-linearly correlated with XRF intensities throughout sediment cores, due to matrix effects, physical properties, and geometry of the sample in different sections. To avoid such effects, we resort to using log ratios of  $\mu\text{-XRF}$  intensities, which are linear functions of log ratios of element concentrations (Weltje and Tjallingii, 2008). The log-ratio transformation also helps with issues related to closed-sum data encountered in multivariate statistical analyses (Martin-Puertas et al., 2017).

### Stable isotope analysis

Organic carbon (C) and nitrogen (N) concentrations and standard isotopic ratios ( $\delta^{13}\text{C}$ ,  $\delta^{15}\text{N}$ ) were measured on dried bulk sediment samples every 10 cm for the Fox Lake sediment core and every 5 cm for the Devils Lake sediment cores. Analyses were conducted at the Stable Isotope Mass Spectrometry Laboratory at Kansas State University and the Central Appalachian Stable Isotope Facility at the University of Maryland following standard procedures for sediment samples. To maximize precision, in-house standards calibrated to PeeDee Belemnite ( $\delta^{13}\text{C}$ ) and atmospheric  $\text{N}_2$  gas ( $\delta^{15}\text{N}$ ) were used. Analytical error was better than 0.1‰ for  $\delta^{13}\text{C}$  and better than 0.2‰ for  $\delta^{15}\text{N}$ . The C:N ratio of the bulk sediment was calculated by dividing %C by %N.

### Particle size analysis

Bulk sedimentary particle size was measured for Fox Lake sediments because of an expectation that particle size would change during the Holocene as aridity and eolian inputs changed. We did not measure particle size with this method at Devils Lake because of the nature of the sedimentary material and difficulty in interpreting bulk particle size in this depositional environment. Throughout the 9.3-m Fox Lake sediment core, 1 mL samples were removed from every third centimeter. Each sample was pretreated with 30 mL of 25%  $\text{H}_2\text{O}_2$  at 80°C to remove organic matter. After settling overnight, excess liquid was decanted. Samples were measured using a laser particle size analyzer through a wet dispersion unit (Mastersizer 3000 and Hydro EV accessory; Malvern Instruments, Worcestershire, UK). The analyzer outputted volume percentages for 100 size classes from 0.01 to 3500  $\mu\text{m}$ . Volume percentages from these size classes were summed according to United States Department of Agriculture (USDA) grain size categories: clay <2  $\mu\text{m}$ ; silt, 2–50  $\mu\text{m}$ ; sand, 50–2000  $\mu\text{m}$ ; and gravel, >2000  $\mu\text{m}$ . While most sediments are finer-grained than soils, we used the USDA classification to match interpretations of particle size transport.

### Magnetic parameters and unmixing model

To gain insight into sediment dynamics at Devils Lake we calculated the fluxes of lithogenic (LITH), pedogenic (PED), and biogenic (BIO) magnetic minerals using the method developed by Lascu et al. (2010). For this we

measured anhysteretic remanent magnetization (ARM), saturation magnetization ( $M_s$ ), and saturation remanent magnetization ( $M_{rs}$ ) at the Institute for Rock Magnetism, University of Minnesota. A D-Tech 2000 demagnetizer was used for the acquisition of ARM in a 0.1 mT direct field superimposed on an alternating frequency field decaying at a rate of 5  $\mu$ T per half cycle from a peak value of 200 mT. ARM susceptibility ( $\chi_{ARM}$ ) was calculated by dividing the ARM to the direct field. Remanence measurements were performed using a 2G superconducting rock magnetometer.  $M_s$  and  $M_{rs}$  were obtained from slope-corrected hysteresis loops measured on a Princeton Measurements vibrating sample magnetometer using a maximum applied field of 1 T and a step size of 5 mT.

Using the unmixing model of Lascu et al. (2010), we derived relative abundances and fluxes of three magnetic components in the sediments from the magnetic measurements. The BIO, PED, and LITH components were determined to be the end members in the unmixing model, based on their distinct values for the ratios of  $M_{rs}/M_s$  and  $\chi_{ARM}/M_{rs}$  (0.5 and 1.5 mm/A for BIO; 0.2 and 0.01 mm/A for PED; and 0.05 and 0.01 mm/A for LITH). The BIO end member represents a population of grains with narrow size range (30–80 nm) produced in the lake by magnetotactic bacteria, via controlled biomineralization of magnetite, a process that entails alignment of the nanocrystals in chains. After the death of the bacteria, these particles are preserved in the sediment as magnetofossils (either as linear or partially collapsed chains), and provide information about the physical and geochemical conditions in the lake. The PED end member

originates in the catchment soils, as the result of magnetic enhancement either through abiotic precipitation, or induced biomineralization by dissimilatory iron-reducing bacteria. The pedogenic ensemble comprises clustered grains of magnetite ranging in size from a few nm to 1–2  $\mu$ m, and are transported to the lake by surface runoff. The LITH end member is representative of magnetic particles in the silt grain-size range. The source of these larger particles is in the bedrock, and transport to the lake is accomplished by streams and/or overland flow. Fluxes of each end member were calculated as magnetite ( $M_s = 92 \text{ Am}^2/\text{kg}$ ) by multiplying the relative abundance by the fraction of dry sediment, gamma density from core logging, and sediment accumulation rate from the age model (Lascu et al., 2010). We did not measure magnetic properties of Fox Lake sediments with this method because of differences in parent material and associated uncertainties in interpretation of magnetic data.

**Table 2.** The 21 input variables for the principal component analysis of the Devils Lake sediment core and eigenvectors for each variable on the first two principal components.

	Principal component 1	Principal component 2
Charcoal count	0.17	0.63
Ca	0.92	-0.24
Sr	0.62	-0.50
K	0.91	-0.22
Fe	0.67	0.12
Mn	0.85	0.16
Si	0.87	0.07
S	-0.15	-0.56
Ti	0.76	-0.35
$\delta^{15}\text{N}$	0.13	0.86
N (%)	-0.89	-0.23
$\delta^{13}\text{C}$	-0.73	-0.31
C (%)	-0.90	-0.07
Flux LITH ( $\mu\text{g}/\text{cm}^2/\text{yr}$ )	0.77	-0.24
Flux PED ( $\mu\text{g}/\text{cm}^2/\text{yr}$ )	0.69	-0.23
Flux BIO ( $\mu\text{g}/\text{cm}^2/\text{yr}$ )	0.11	-0.18
Flux total ferrimagnetic ( $\mu\text{g}/\text{cm}^2/\text{yr}$ )	0.78	-0.25
<i>Picea</i>	0.87	-0.18
<i>Quercus</i>	-0.83	-0.32
<i>Ulmus</i>	-0.13	0.78
Poaceae	0.33	-0.54

### Multivariate statistics

To investigate if the terrestrial biosphere determined the trajectory of elemental change, principal component analyses were performed on the eight elemental counts derived from XRF, as well as additional variables capturing different aspects of ecosystem history for Fox Lake and for Devils Lake. There were a total of 21 input variables for Devils Lake (Table 2) and 17 variables for Fox Lake (Table 3). The number of variables differed between the sites due to: (1) differences between magnetic and particle size parameters measured on the sediments of each lake, and (2) differences in the number of pollen variables required to summarize vegetation change between the grassland and forested sites. All variables for Fox Lake and all variables for Devils Lake except

**Table 3.** The 17 input variables for the principal component analysis of the Fox Lake sediment core and eigenvectors for each variable on the first two principal components.

	Principal component 1	Principal component 2
Magnetic susceptibility (SI)	0.06	0.83
Arboreal pollen (%)	0.17	-0.57
Flux clay ( $\text{mg cm}^2/\text{yr}$ )	0.37	-0.34
Flux sand ( $\text{mg cm}^2/\text{yr}$ )	-0.15	-0.17
$\delta^{15}\text{N}$	-0.40	-0.05
N (%)	0.40	-0.78
$\delta^{13}\text{C}$	-0.40	0.82
C (%)	0.30	-0.76
Ca	0.85	-0.13
Sr	0.88	-0.16
K	0.93	-0.20
Fe	0.78	-0.30
Mn	0.49	0.70
Si	0.88	-0.24
S	0.65	-0.50
Ti	0.85	-0.24
Charcoal count	0.15	-0.29

for pollen were measured on the 2012 core. Pollen data were correlated to the 2012 core using the age model of Grimm et al. (2009) and the age model of Williams et al. (2015). The analyses were performed on the correlations because the units differed among the input variables, and data were statistically resampled to the lowest resolution by depth for all variables (every 5 cm for Devils Lake and every 10 cm for Fox Lake). Principal components were rotated to strengthen contrasts.

## RESULTS

### Sediment sources

The source material analysis at the forested site (Devils Lake) is based on the magnetic end member fluxes from the unmixing model and the C:N ratio (Fig. 2). The non-biogenic magnetic material input changed over time, with gradual declines in fluxes of both LITH and PED toward present, except for an increase in both components between ~5000 and 3000 cal yr BP. PED fluxes also increased between ~9000 and ~7000 cal yr BP. Magnetofossil flux (BIO) was relatively constant for most of the record, except in the sediments deposited during the past several centuries, when the flux increased by an order of magnitude. The source of the organic matter seems to be aquatic, as evidenced by C:N values that rarely exceeded 10, the ratio found in aquatic microbes and algae.

Source material variability during the course of system development at the grassland site (Fox Lake) was evaluated via sediment grain-size analyses and the C:N ratio (Fig. 3).

Throughout the record, the flux of silt was dominant, with sand being secondary in importance. Comparatively, only very small amounts of clay were delivered to the sediments for most of the record. Two important shifts should be highlighted: (1) a striking increase in influx of sand-sized particles during the Mid-Holocene around 5500 cal yr BP (zone F3), and (2) an increase in clay and silt influx starting at 1500 cal yr BP (zone F1). The C:N ratio in Fox Lake was almost exclusively >10, indicating that the organic matter was mainly sourced within the catchment. The steady decline of C:N values throughout the Holocene suggests either decreasing terrestrial plant inputs, or an increase in relative abundance of algae and aquatic bacteria (Fig. 3).

### Sediment geochemistry

To study the sequence of ecosystem processes at each site, we examined temporal patterns of XRF-derived relative elemental abundance. At the forested site  $Ti_{clr}$ ,  $K_{clr}$ ,  $Si_{clr}$ , and  $Ca_{clr}$  were highest in zone D5, then declined during the late glacial, followed by relatively constant values throughout the Holocene, until ~500 cal yr BP (Fig. 4a).  $Fe_{clr}$  and  $Mn_{clr}$  reached maxima in zone D4, before decreasing throughout the record starting with the Younger Dryas (ca. 12,750 cal yr BP; Hughen et al., 2000).  $Ti_{clr}$ ,  $K_{clr}$ ,  $Si_{clr}$ ,  $Ca_{clr}$ , and  $Fe_{clr}$  reached their Holocene maxima during the first part of the Holocene hypsithermal, between ca. 9500 and 7000 cal yr BP (Dean et al., 1997).  $S_{clr}$  experienced a steady increase throughout the record. Element abundances increased in the last few centuries of the record (zone D1). Log ratios of Ti-normalized

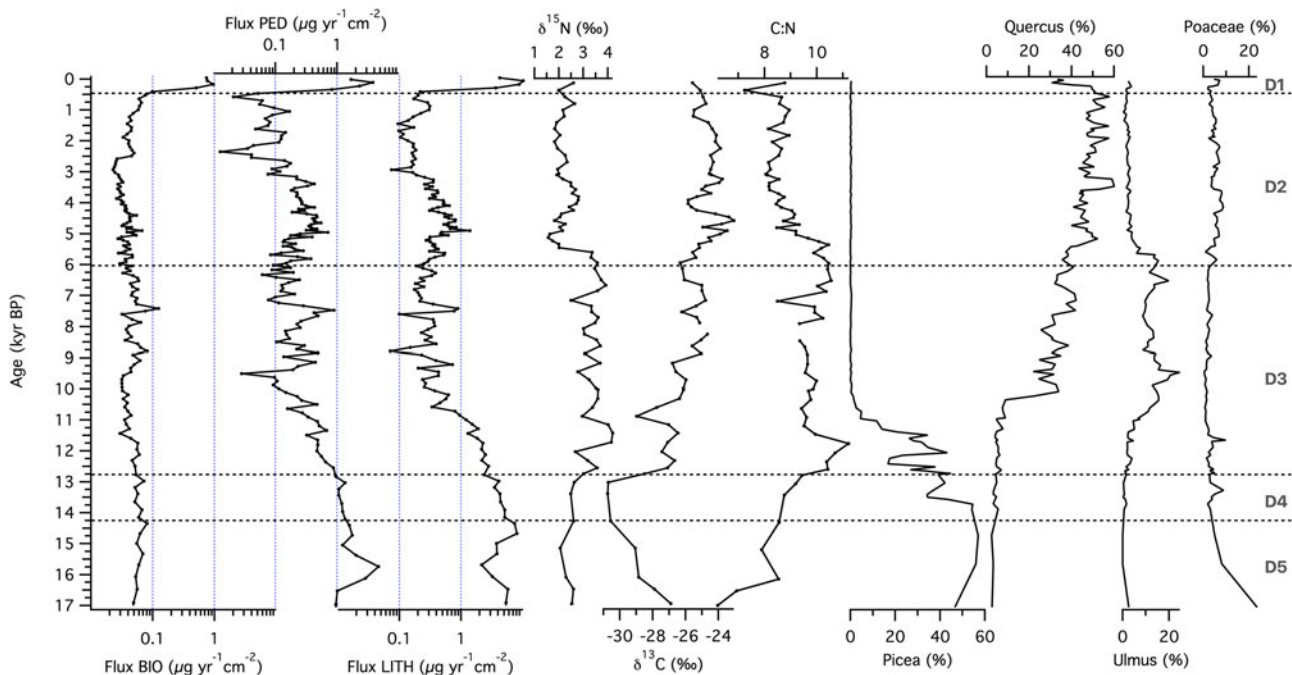


**Figure 2.** Source material of sediments at the forested site (Devils Lake, Wisconsin): fluxes of biogenic (BIO), pedogenic (PED), and lithogenic (LITH) ferrimagnetic material calculated from measured magnetic parameters, N and C isotopic composition, and C:N ratio of organic material, and relative abundances of main pollen types. Zones (D1–D5) were based on lithologic transitions in the sediment core identified by Williams et al. (2015).

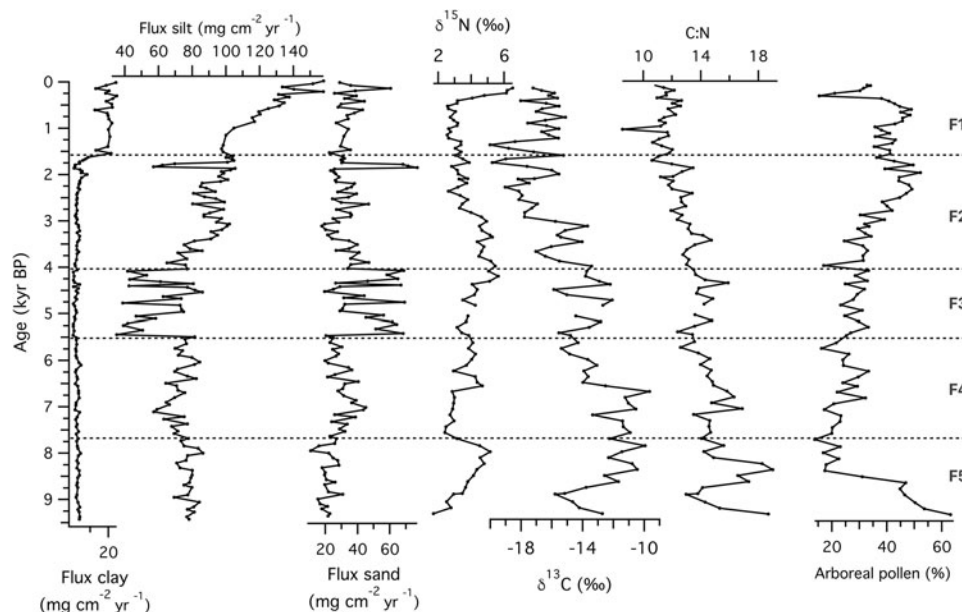


**Figure 3.** Source material of sediments at the grassland site (Fox Lake, Minnesota): fluxes of clay, silt, and sand, N and C isotopic composition, and the C:N ratio of organic material, and relative abundance of arboreal pollen. Zones (F1–F5) were based on magnetic susceptibility transitions in the sediment core identified by Commerford et al. (2016).

elemental counts are shown in Figure 4b.  $\ln(K/Ti)$  and  $\ln(Si/Ti)$  demonstrated a pattern of decline toward present, with  $\ln(K/Ti)$  exhibiting a stronger gradient across the Pleistocene-Holocene transition.  $\ln(Ca/Ti)$  values were variable but high in zones D5 and D4, then underwent a sharp transition at  $\sim 12,750$  cal yr BP, followed by a decrease until 8000 cal yr BP. A local maximum between 8000 and 7000 cal yr BP is followed by relatively constant values for the rest of the record.  $\ln(Fe/Ti)$  and  $\ln(Mn/Ti)$  displayed increasing values until  $\sim 9000$  cal yr BP, with local maxima in zones D5 (for Mn) and D4 (for Fe and Mn). Both  $\ln(Fe/Ti)$  and  $\ln(Mn/Ti)$  displayed pronounced maxima occurred during the Early Holocene ( $\sim 11,500$ – $9000$  cal yr BP).  $\ln(S/Ti)$  showed an oscillatory pattern but increased over time toward present.

Relative elemental abundances in sediments from the grassland site demonstrated a similar pattern to those from the forested site during the Holocene. All seven selected elements demonstrated a long-term decline in abundance from the beginning of the record to present (Fig. 5). This was not a monotonic decline, however. During the early portion of the record (from 9200 to  $\sim 8500$  cal yr BP, zone F5), when Fox Lake was surrounded by oak woodland, abundances initially increased, with all elements except  $S_{clr}$  exhibiting the highest values in the record at the transition to grassland (ca. 8500 cal yr BP). Other notable peaks occurred in zone F4 ( $Ca_{clr}$  and  $S_{clr}$ ) and around 4000 cal yr BP ( $Ti_{clr}$ ,  $K_{clr}$ ,  $Si_{clr}$ ,  $Ca_{clr}$ ,  $Fe_{clr}$ , and  $S_{clr}$ ). Log ratios of Ti-normalized counts again revealed different patterns from the absolute counts, with  $\ln(K/Ti)$  and  $\ln(Si/Ti)$  declining,  $\ln(Mn/Ti)$  and  $\ln(Fe/Ti)$  increasing, and  $\ln(S/Ti)$  and  $\ln(Ca/Ti)$  exhibiting variable behavior, with Mid-Holocene maxima.

Temporal changes in source material and geochemical structure of sediments can be analyzed with relationships

among selected elements. At the forested site, there were positive correlations between  $Si_{clr}$  and  $K_{clr}$  ( $R=0.91$ ),  $K_{clr}$  and  $Fe_{clr}$  ( $R=0.66$ ),  $Mn_{clr}$  and  $Fe_{clr}$  ( $R=0.77$ ), and  $Ca_{clr}$  and  $Sr_{clr}$  ( $R=0.76$ ), although the correlation strength varied with time (Fig. 6). Slope changes, such as the ones observed in the  $K_{clr}$ - $Fe_{clr}$  or  $Ca_{clr}$ - $Sr_{clr}$  biplots, indicate temporal variability in geochemical processes. Relationships among elemental counts at the grassland site showed similar positive correlations (Fig. 7), which were very strong throughout the entire record for  $Si_{clr}$  and  $K_{clr}$  ( $R=0.97$ ), and  $K_{clr}$  and  $Fe_{clr}$  ( $R=0.96$ ). These two relationships were linear with very little scatter, suggesting similar source material or processes throughout the history of sediment deposition. For  $Mn_{clr}$  and  $Fe_{clr}$  and  $Ca_{clr}$  and  $Sr_{clr}$  the correlation was still strong ( $R=0.85$  and  $0.81$ , respectively), but exhibiting more scatter.

### Principal component analyses

At the forested site (Fig. 8), the first principal component, explaining 47.7% of the variability in the dataset, followed the stratigraphic trend that showed a major transition from minerogenic to organic-rich sediments after 13,000 cal yr BP (D4-D3 transition). Samples with high values of elemental counts, LITH and PED fluxes, and *Picea* pollen loaded positively on the first principal component, while samples with high values of  $\delta^{13}C$ , C and N concentrations, and *Quercus* pollen loaded negatively on the first principal component. The second principal component, explaining 16.1% of the variability, separated samples high in *Ulmus* pollen, charcoal, and  $\delta^{15}N$  from samples high in Poaceae pollen and S concentration.

At the grassland site (Fig. 9), the first principal component, explaining 34.8% of the variability in the dataset, displayed

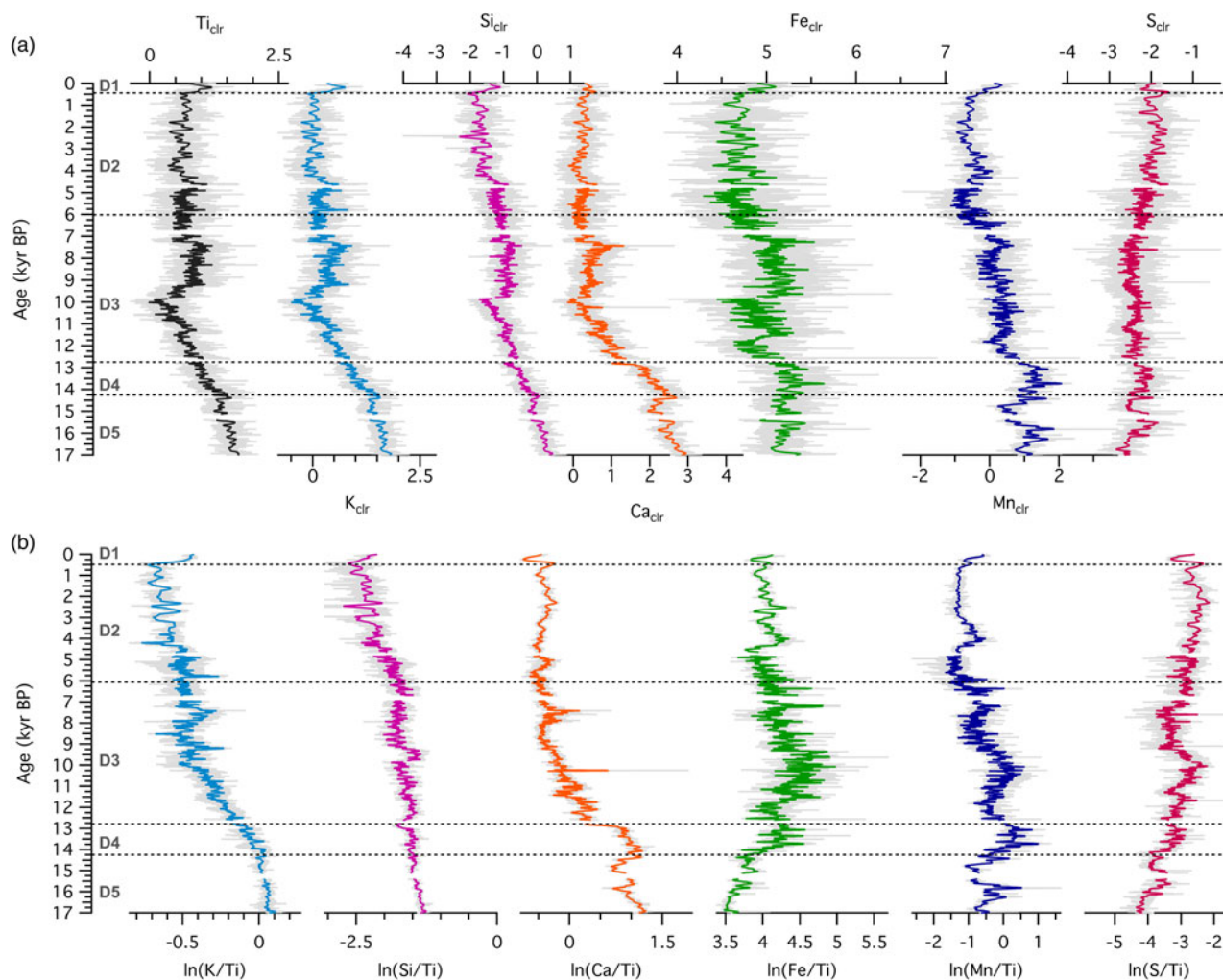


**Figure 4.** (color online) (a) Centered-log ratios of selected elements and (b) log ratios of element intensities with respect to the intensity of Ti for sediments from the forested site (Devils Lake, Wisconsin).

periods of little change (e.g., in zone F4), continual decrease (e.g., in zone F3), and continual increase (e.g., in zone F2). Samples with high values of elemental counts loaded positively on the first principal component, and samples with high values of  $\delta^{15}N$  and sand loaded negatively on the first principal component. The second principal component, explaining 24.3% of the variability, separated samples high in arboreal pollen types and C and N concentrations from samples with high magnetic susceptibility, Mn concentrations, and  $\delta^{13}C$  values.

## DISCUSSION

### How did source material change over time?

Source materials at both sites changed as evidenced in the sedimentary sequences. At Fox Lake, progressively lower values of C:N reflect gradually declining terrigenous organic inputs and a shift to a predominance of aquatic algal and bacterial organic matter. A similar pattern was observed at

Deming Lake, 425 km to the north of Fox Lake (Fig. 1), with reduced fluxes of both terrestrial organic material and total sediment deposition over the entire 9500-yr sequence (McLauchlan et al., 2013). The mineral matter flux at Fox Lake increased over time, with the proportion of sand gradually decreasing (except for a transient increase between 5500 and 4000 cal yr BP) in favor of silt and clay, especially for the last 1500 yr.

At Devils Lake, mineral sediment sources shifted from inputs from bedrock sources, as indicated by the pre-Holocene predominance of lithogenic magnetic particles, to catchment soils- and lake-derived material, reflected by increasing amounts of pedogenic and biogenic magnetic particles toward present. A noted exception was the increase of both PED and LITH fluxes during the Mid-Holocene, a warm and dry interval. Several sedimentary records in the region indicate increased eolian influx during this time, such as increased quartz inputs at Elk Lake, Minnesota (Dean, 1997). Small inputs of calcareous loess have been noted at Devils Lake during the Mid-Holocene from sources to the west (Grimm et al., 2009). While this would be barely



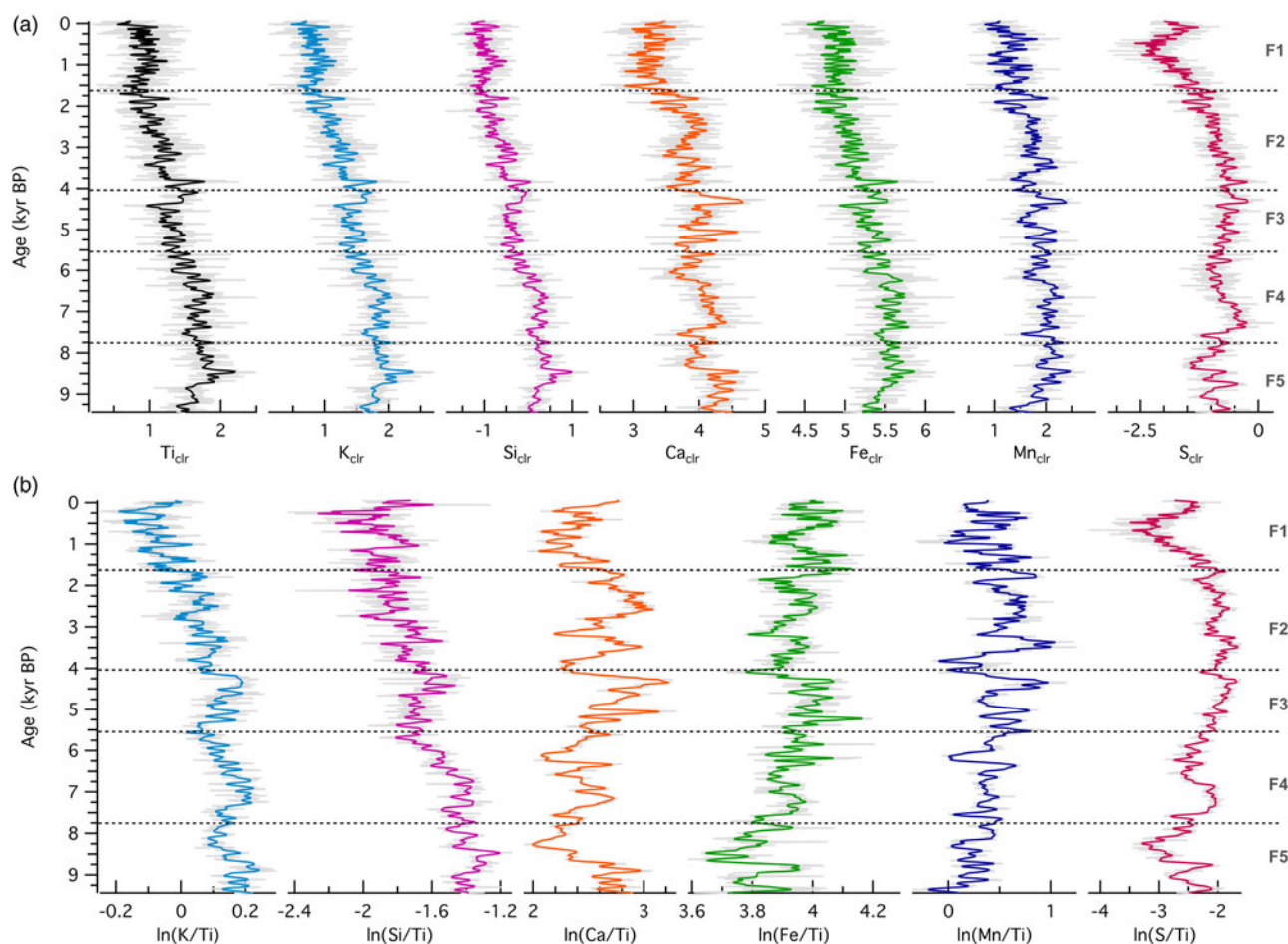


**Figure 5.** (color online) (a) Centered-log ratios of selected elements and (b) log ratios of element intensities with respect to the intensity of Ti for sediments from the grassland site (Fox Lake, Minnesota).

detectable in XRF data as elevated Ca levels, magnetic parameters provide more detail about eolian inputs depending on the size of the wind-blown particles. If they are in the very fine silt size range (2–4  $\mu\text{m}$ ), they contribute to the PED component, whereas if they are larger they contribute to LITH fluxes. Abrupt increases in sand influx beginning at 5500 cal yr BP at Fox Lake reflected the proximity to dune fields to the south that mobilized around the same time during increased aridity (Miao et al., 2006).

### What were the nutrient patterns during Holocene ecosystem development?

While different lengths of time are represented in the records presented here—9200 yr for Fox Lake and 17,000 yr for Devils Lake—the similarity in geochemical patterns indicates that the sequence of processes may be the same across sites although the rate of these processes may vary. Temporal patterns of accumulation of nutrients in the sediments, especially N and base cations, during Holocene ecosystem development indicate striking secular trends. One of the strongest patterns in these records is the slow decline in elemental abundances toward present, reflecting some kind of ontogenetic process or combination of processes. This is especially interesting

given the different lithologic settings of these two sites, and the relatively heterogeneous nature of glacial till present on both sites. Lakes in pure bedrock settings, especially basalt and granite with well-established weathering pathways, may demonstrate even clearer signals of geochemical change over time (Sperber et al., 2017; Burghelca et al., 2018)

Similar patterns—declines in concentrations of easily weathered elements such as Ca and Sr—have been documented in late-Pleistocene and Holocene sedimentary records in the Alps (Koinig et al., 2003; Schmidt et al., 2006) and the southern Urals (Maslennikova et al., 2016). Clear signals of N accumulation, as seen in chronosequences (Engstrom et al., 2000; Wardle et al., 2004) and some lake sedimentary sequences (Hu et al., 2001; McLauchlan et al., 2013), are also seen at Fox Lake in sedimentary  $\delta^{15}\text{N}$  (Fig. 3). An increase in  $\delta^{15}\text{N}$  values at the beginning of the sedimentary record was not as clear at Devils Lake, possibly due to climatic control of N fluxes to the basin during ice sheet retreat and very early landscape evolution (Williams et al., 2015). It is possible, however, that additional factors confound interpretation of  $\delta^{15}\text{N}$  values as indicating early successional processes.

The relationships between elements show dominantly, but not entirely, abiotic control of elemental ratios. At Fox Lake,

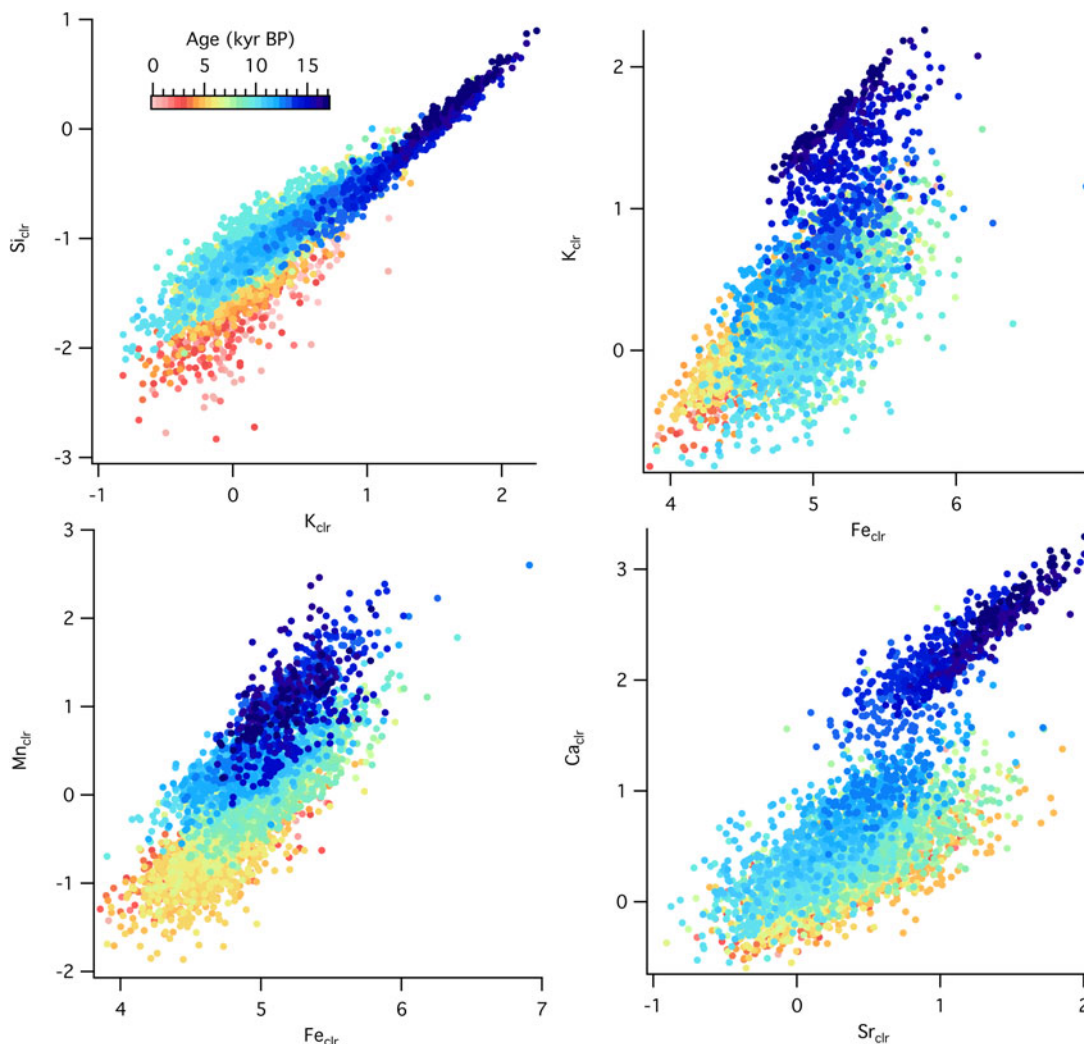


**Figure 6.** (color online) Cross plots of selected element abundances from the sedimentary sequence at the forested site (Devils Lake, Wisconsin) color coded by time.

$K_{\text{clr}}$  and  $Ca_{\text{clr}}$  both decline from 8000 yr toward present, a time period when grassland vegetation stayed relatively constant (Fig. 5). Si, K, Ti, and Ca abundances in Devils Lake show similar decreasing trends over the first 7000 yr of the record. In the bedrock present at this site, K and Ca are found in extremely low concentrations, as the Baraboo quartzite is both chemically and physically mature (Medaris et al., 2003). The quartzite and the claystone and siltstone layers interspersed within the quartzite are composed of Si, Ti, Al, and Fe (Medaris et al., 2003). Early inputs of K and Ca to Devils Lake may have been either from unstable, sparsely vegetated local catchment sources deposited by the retreating glacier, which have subsequently been eroded or chemically weathered, or increased eolian deposition due to drier conditions. Maximum K and Ca abundances in Devils Lake between 9500 and 7000 cal yr BP are more difficult to interpret, as they occur in the middle of zone D3 when vegetation composition is fairly stable. Subsequent stabilization of the catchment has reduced clastic input in the lake and abundances of Ca and K have leveled off after 7000 cal yr BP.

In Devils Lake zone D4,  $\ln(Ca/Ti)$  increased, in contrast to  $\ln(K/Ti)$  and  $\ln(Si/Ti)$ , which coincided with peaks in  $\ln(Mn/Ti)$ ,  $\ln(Fe/Ti)$ , and  $\ln(S/Ti)$ . These patterns in ratios could be related to a shift to endogenic mineral precipitation, likely due to a change in the redox state of the lake waters in response to climate change during the late glacial interstadial. During this time period, dark, banded microbial sediments were accumulating in deep, stratified lake waters characterized by bottom anoxia (Williams et al., 2015).  $\ln(Ca/Ti)$  decreased suddenly with abrupt cooling at the onset of the Younger Dryas. Throughout the record, the decline in  $\ln(Si/Ti)$  lagged behind  $\ln(K/Ti)$ , which in turn lagged behind the decline in  $\ln(Ca/Ti)$ , as Ca is more easily mobilized than K during chemical weathering, and Si is the least prone to be dissolved (Nesbitt et al. 1996).  $\ln(Si/Ti)$  was high at the beginning of the record and decreased afterward, suggesting that initial inputs of lithogenic silica from the catchment during glacial retreat were extremely high. As the catchment stabilized, physical weathering decreased and detrital input decreased. Peaks in  $\ln(Si/Ti)$  at  $\sim 9,500$  cal yr BP and to a lesser extent

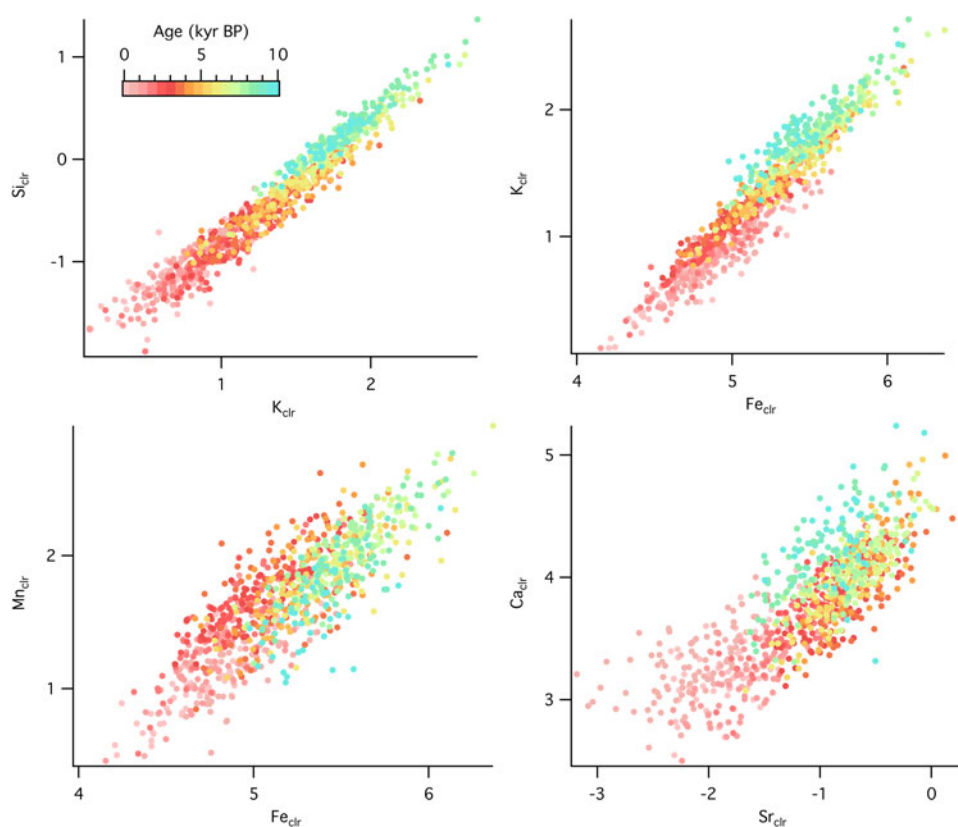


**Figure 7.** (color online) Cross plots of selected element abundances from the sedimentary sequence at the grassland site (Fox Lake, Minnesota) color coded by time.

at ~6,500 cal yr BP, may suggest increased contributions from biogenic silica at those times. Despite the appearance of diatoms and corresponding in-lake productivity around 7500 cal yr BP, biogenic silica inputs were not as large as the previous high input of detrital silica.

Fe is correlated to both K and Ti throughout the record at both sites, suggesting that Fe in the lake sediments is mainly detrital. There are time periods characterized by weaker correlation between Fe and K and Fe and Ti, however, especially at the forested site. This points to a more important contribution from authigenic iron-bearing minerals, meaning Fe entered the lake in dissolved form through ground water and precipitated as iron oxides and/or hydroxides. High  $\ln(\text{Fe}/\text{Ti})$  and  $\ln(\text{Mn}/\text{Ti})$ , along with abundant vivianite and pyrite in zone D4 (visually identified using petrography), suggest reducing conditions during the late glacial interstadial (Williams et al., 2015). At the grassland site, the S trend correlates with those of the other elements, suggesting an origin from sulfates in the calcareous tills from the catchment (Gorham et al., 1983). At the forested site, S has an opposite trend to the other elements, suggesting it is associated with organic matter, which increases steadily throughout the record (Williams et al., 2015).

The Ca-Sr relationship provides additional information about the source material. Concentrations of Ca and Sr in the Baraboo quartzite are extremely low (Medaris et al.,

2003), while the till around Fox Lake is calcareous (Commerford et al., 2016). Sr often substitutes for Ca in calcium-bearing minerals and is equally mobile during chemical weathering. At Fox Lake,  $\ln(\text{Ca}/\text{Sr})$  is higher during the oak woodland phase prior to 8200 cal yr BP and lower during the grassland phase after 8200 cal yr BP. At Devils Lake,  $\ln(\text{Ca}/\text{Sr})$  is high prior to 12,800 cal yr BP and low and relatively constant from 12,800 cal yr BP to present (Fig. 6). Strong correlation between Ca and Sr indicates a single source for both elements, while a weaker correlation suggests separate provenance, e.g., Ca from an endogenic source and Sr from a lithogenic source.

Climate conditions—hydrologic changes in the catchment, lake level, and evaporation—were considered in other studies to strongly influence elemental concentrations of same seven elements that we studied here (Martin-Puertas et al. 2011; Heymann et al., 2013). Lithological composition and mineralogy (quartz silicates, clay silicates, calcite, and coarse particles) have also been considered the dominant factor in determining sedimentary elemental concentrations (Koinig et al., 2003). Declines in elemental concentration could be simply reflecting depletion of mobile elements such as Ca and K from source material in the catchment (Minyuk et al., 2014). In addition to simple first order hydrologic dissolution, there could be a change in the pace of chemical or physical weathering, or changes in transport pathways similar

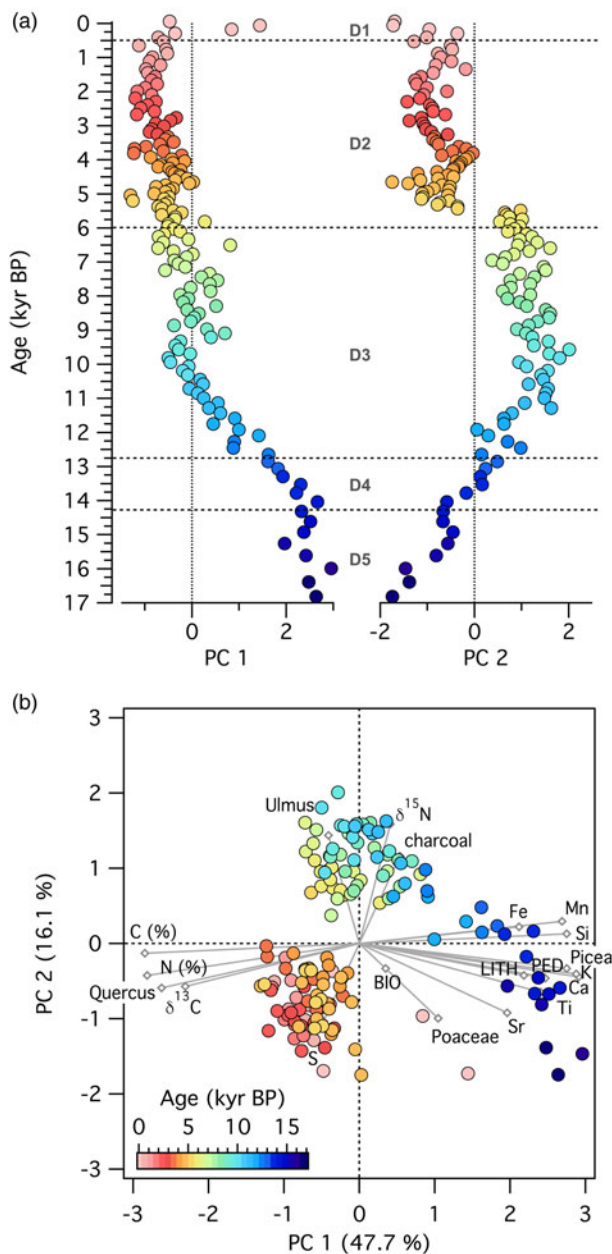


**Figure 8.** (color online) Principal components analysis of 21 variables measured on a sediment core spanning the entire sequence of ecosystem development following deglaciation ~17,000 yr from Devils Lake, Wisconsin. (a) Time series of principal components 1 and 2. (b) Score plot of principal components 1 and 2. Circles, data points; diamonds, eigenvectors for each of the variables.

to those observed in Glacier Bay, Alaska during ecosystem development (Milner et al., 2007). Recently, a unified “erosion signal” has been identified in alpine lake sediments characterized by changes in elemental concentrations (Arnaud et al., 2016). In lacustrine settings, Ti is considered a metric of detrital input, so a decline in Ti concentration as observed at both sites in this study likely indicates a gradual decline in detrital input. Finally, there could be further influences through the mechanism by which elements are precipitated in sediments and diagenetic alteration.

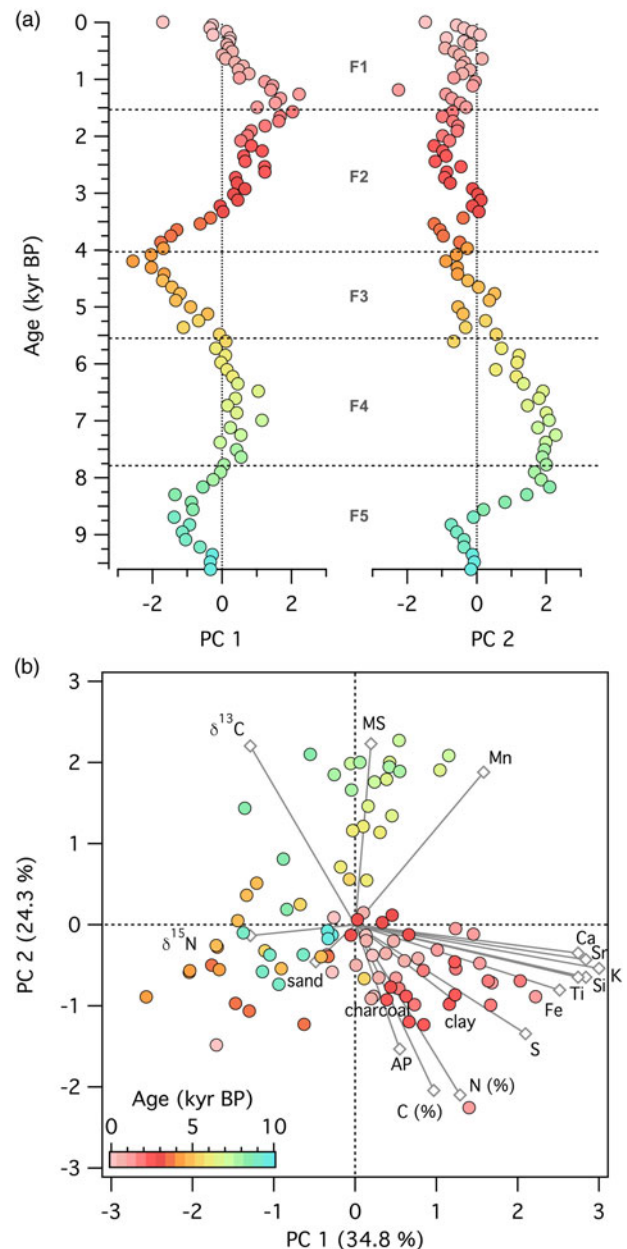


**Figure 9.** (color online) Principal components analysis of 17 variables measured on a sediment core spanning 9200 yr of ecosystem development following deglaciation from Fox Lake, Minnesota. (a) Time series of principal components 1 and 2. (b) Score plot of principal components 1 and 2. Circles, data points; diamonds, eigenvectors for each of the variables.

### Biosphere-lithosphere interactions: did vegetation determine the trajectory of elemental change at each site?

After initial establishment of vegetation at each site, comparisons of vegetation and geochemical change between sites indicate a limited role of vegetation change in influencing geochemical parameters at each site. This generally agrees with other studies that attribute changes in element concentrations in sediment cores to climate-driven changes in

weathering and transport processes. An alternative possibility is sediment geochemical change should be attributed to climate-driven vegetation change and subsequent changes in biogeochemical cycling (Martin-Puertas et al., 2017). In our study, at both the grassland site and the forested site, the first principal component separated samples with high elemental abundances from those with high organic matter concentration. At the forested site, high *Picea* pollen loaded positively on the first axis with the elemental counts, and *Quercus* pollen loaded with organic matter, but this is difficult to interpret purely as a vegetation signal due to a simultaneously warming climate. Thus, there was some correlation of elemental change and forest composition (either hardwood or coniferous forest), but there was also concurrent climate change occurring over the intervals with changes in forest composition.

The other vegetation transitions later in the Holocene at the forested site (involving *Ulmus*) are only correlated with  $\delta^{15}\text{N}$ , which indicates strong links between vegetation and N cycling throughout the record. Arboreal pollen at Fox Lake and Poaceae (non-arboreal pollen) at Devils Lake loaded in the opposite direction from the N-cycling proxy  $\delta^{15}\text{N}$  at both sites. Early Holocene vegetation reorganization and development of the lake catchment played dominant roles in sediment deposition at Lake Meerfelder Maar, Germany (Martin-Puertas et al., 2017). Interactions among vegetation types were important during the transition from glacial to interglacial conditions at the Gerzensee site in Switzerland (Ammann et al., 2013), but this may be due to the relatively large magnitude of vegetation change as indicated in pollen assemblages.

The degree of vegetation change in this study, while notable at each site, is not as large as those demonstrated to cause geochemical changes in other sequences between glacial and interglacial conditions. In particular, differences in primary productivity during stadial-interstadial cycles caused changes in weathering rates at Les Échets, France (Kylander et al., 2011), and Lake El'gygytgyn, Russia (Minyuk et al., 2014). The onset of aquatic productivity and organic matter deposition was certainly important at Devils Lake, resulting in anoxic conditions and notable black bands dominated by amorphous aquatic organic material in the sediments (Williams et al., 2015). While the rate of declining elemental concentrations was altered significantly by this one transition from glacial to interglacial conditions, however, the direction of the trajectory was the same across the transition, indicating a more complex set of processes in addition to plant colonization of a bare landscape. In early succession on recently deglaciated terrain, the timing of establishment of certain plant functional types such as  $\text{N}_2$  fixers and coniferous trees can have significant effects on accretion of soil C and N, and erosion rates (Crocker and Major, 1955; Fastie, 1995). At Devils Lake, the transition from coniferous to deciduous forest in zone D3 certainly affected fire regime, but not the geochemistry based on the Ti-normalized element concentrations. Finally, geochemical sedimentary records may be able to add detail to the classic view that the relative importance of

autogenic and allogenic processes changes over successional time (Matthews, 1992).

Another way to assess the role of the terrestrial biosphere is to compare the trajectories between the two sites. The similarities in the sequence of geochemical changes between the forest and the grassland site provide further support for a limited role of vegetation type. Comparisons of absolute rates of change are complicated by different elemental counts between sites, but, for example, declines in  $\ln(\text{K}/\text{Ti})$  and  $\ln(\text{Ca}/\text{Ti})$  seem to be faster at the forested site than at the grassland site. Differences in lithology, topography, and basin size, however, could be more important than vegetation differences between grassland and forest. In particular, Fox Lake is larger and shallower, with calcareous glacial till as parent material and significant agricultural land use in the watershed. Devils Lake is deeper, with non-calcareous glacial till and Precambrian quartzite as parent material and a protected watershed within a state park. As an alternative hypothesis, it is possible that climate change was directly influencing geochemistry through catchment weathering and hydrologic transport of material into the lake basin. Further estimates of weathering rates, catchment destabilization due to aridity, or hydrologic fluxes over Holocene timescales would help test these hypotheses.

## CONCLUSIONS

To assess rates, patterns, and mechanisms of ecosystem development after glacial retreat, we compared two sedimentary sequences in the upper Midwestern United States, one from a grassland site and a forested site. We found that source material changed over the Holocene sedimentary sequences. We also found that the patterns of nutrients, especially limiting nutrients such as N, K, Ca, and Mg, changed over the Holocene sedimentary sequences. It seems that once vegetation was established, there was minimal influence of vegetation composition on inorganic sediment properties thereafter. At the forested site, transitions among vegetation from *Picea* to *Pinus* to deciduous hardwood led to changes in fire regime and nutrient cycling but not inorganic element abundances. At the grassland site, the transition from oak forest to grassland affected primarily delivery of organic material to the catchment. There is future potential to interpret sedimentary elemental concentrations in light of ecological processes. Two aspects are likely to make these successful: (1) comparing several sites with different vegetation histories, and (2) measuring many proxies to help provide independent estimates of multiple processes influencing sediment records.

## ACKNOWLEDGMENTS

We thank J. Mueller, S. McConaghy, J. Commerford, A. Myrbo, K. Brady, A. Lingwall, T. Ocheltree, R. Paulman, and R. Keen for field and laboratory assistance. J. L. Morris provided helpful discussion about the Fox Lake XRF data. We thank Catherine Yansa and an anonymous reviewer for comments that greatly improved the manuscript. Financial support was provided by National Science

Foundation BCS-0955225 to K.M. and a Kansas State University College of Arts and Sciences Undergraduate Scholarship to R.S. Support for I.L. was provided through ERC grant 320750 under the European Union's Seventh Framework Programme (FP/2007-2013). KM managed the project and led manuscript preparation. IL led data analysis and figure conception. IL, EM, and KM led data interpretation. All authors generated primary data from Fox Lake and/or Devils Lake sediment cores, and all authors discussed results and contributed to manuscript preparation.

## REFERENCES

- Ammann, B., van Raden, U.J., Schwander, J., Eicher, U., Gilli, A., Bernasconi, S.M., van Leeuwen, J.F.N., et al., 2013. Responses to rapid warming at Termination 1 a at Gerzensee (Central Europe): primary succession, albedo, soils, lake development, and ecological interactions. *Palaeogeography, Palaeoclimatology, Palaeoecology* 391, 111–131.
- Arnaud, F., Poulencard, J., Giguët-Covex, C., Wilhelm, B., Revillon, S., Jenny, J.P., Revel, M., et al., 2016. Erosion under climate and human pressures: An alpine lake sediment perspective. *Quaternary Science Reviews* 152, 1–18.
- Attig, J.W., Hanson, P.R., Rawling, J.E., Young, A.R., Carson, E.C., 2011. Optical ages indicate the southwestern margin of the Green Bay Lobe in Wisconsin, USA, was at its maximum extent until about 18,500 years ago. *Geomorphology* 130, 384–390.
- Boyle, J.F., 2007. Loss of apatite caused irreversible early-Holocene lake acidification. *Holocene* 17, 543–547.
- Bradshaw, E.G., Rasmussen, P., and Odgaard, B.V., 2005. Mid- to late-Holocene land-use change and lake development at Dallund Sø, Denmark: synthesis of multiproxy data, linking land and lake. *Holocene* 15, 1152–1162.
- Buma, B., Bisbing, S., Krapek, J., Wright, G., 2017. A foundation of ecology rediscovered: 100 years of succession on the William S. Cooper plots in Glacier Bay, Alaska. *Ecology* 98, 1513–1523.
- Burghilea, C.I., Dontsova, K., Zaharescu, D.G., Maier, R.M., Huxman, T., Amistadi, M.K., Hunt, E., Chorover, J., 2018. Trace element mobilization during incipient bioweathering of four rock types. *Geochimica Et Cosmochimica Acta* 234, 98–114.
- Colombaroli, D., Gavin, D.G., 2010. Highly episodic fire and erosion regime over the past 2,000 y in the Siskiyou Mountains, Oregon. *Proceedings of the National Academy of Sciences of the United States of America* 107, 18909–18914.
- Commerford, J.L., Leys, B., Mueller, J.R., McLauchlan, K.K., 2016. Great Plains vegetation dynamics in response to fire and climatic fluctuations during the Holocene at Fox Lake, Minnesota (U.S.A.). *Holocene* 26, 302–313.
- Crocker, R.L., Major, J., 1955. Soil development in relation to vegetation and surface age at Glacier Bay, Alaska. *Journal of Ecology* 43, 427–448.
- Cutler, N.A., Belyea, L.R., Dugmore, A.J., 2008. The spatiotemporal dynamics of a primary succession. *Journal of Ecology* 96, 231–246.
- Davis, R.B., Anderson, D.S., Dixit, S.S., Appleby, P.G., and Schauffler, M., 2006. Responses of two New Hampshire (USA) lakes to human impacts in recent centuries. *Journal of Paleolimnology* 35, 669–697.
- Dean, W.E., 1997. Rates, timing, and cyclicity of Holocene eolian activity in north-central United States: Evidence from varved lake sediments. *Geology* 25, 331–334.
- Dunnette, P.V., Higuera, P.E., McLauchlan, K.K., Derr, K.M., Briles, C.E., and Keefe, M.H., 2014. Biogeochemical impacts of wildfires over four millennia in a Rocky Mountain subalpine watershed. *New Phytologist* 203, 900–912.
- Engstrom, D.R., Fritz, S.C., Almendinger, J.E., Juggins, S., 2000. Chemical and biological trends during lake evolution in recently deglaciated terrain. *Nature* 408, 161–166.
- Engstrom, D.R., Hansen, B.C.S., 1985. Postglacial vegetational change and soil development in southeastern Labrador as inferred from pollen and chemical stratigraphy. *Canadian Journal of Botany* 63, 543–561.
- Fastie, C.L., 1995. Causes and ecosystem consequences of multiple pathways of primary succession at Glacier Bay, Alaska. *Ecology* 76, 1899–1916.
- Ford, M.S., 1990. A 10,000 year history of natural ecosystem acidification. *Ecological Monographs* 60, 57–89.
- Gorham, E., Dean, W.E., Sanger, J.E., 1983. The chemical composition of lakes in the North-Central United-States. *Limnology and Oceanography* 28, 287–301.
- Grimm, E.C., Maher, L.J., Nelson, D.M., 2009. The magnitude of error in conventional bulk-sediment radiocarbon dates from central North America. *Quaternary Research* 72, 301–308.
- Hahm, W.J., Riebe, C.S., Lukens, C.E., and Araki, S., 2014. Bedrock composition regulates mountain ecosystems and landscape evolution. *Proceedings of the National Academy of Sciences of the United States of America* 111, 3338–3343.
- Heymann, C., Nelle, O., Dorfler, W., Zagana, H., Nowaczyk, N., Xue, J.B., Unkel, I., 2013. Late Glacial to mid-Holocene palaeoclimate development of Southern Greece inferred from the sediment sequence of Lake Stymphalia (NE-Peloponnese). *Quaternary International* 302, 42–60.
- Hu, F.S., Finney, B.P., Brubaker, L.B., 2001. Effects of Holocene *Alnus* expansion on aquatic productivity, nitrogen cycling, and soil development in southwestern Alaska. *Ecosystems* 4, 358–368.
- Hughen, K.A., Southon, J.R., Lehman, S.J., Overpeck, J., 2000. Synchronous radiocarbon and climate shifts during the last deglaciation. *Science* 290, 1951–1954.
- Jenny, H., 1941. *Factors of soil formation: a system of quantitative pedology*. New York, USA, McGraw Hill.
- Koinig, K.A., Shotyk, W., Lotter, A.F., Ohlendörf, C., Sturm, M., 2003. 9000 years of geochemical evolution of lithogenic major and trace elements in the sediment of an alpine lake - the role of climate, vegetation, and land-use history. *Journal of Paleolimnology* 30, 307–320.
- Küchler, A.W., 1964. Potential natural vegetation of the conterminous United States. In: *The National Atlas of the United States of America*. United States Geological Survey, Washington, DC, pp. 89–92.
- Kylander, M.E., Ampel, L., Wohlfarth, B., Veres, D., 2011. High-resolution X-ray fluorescence core scanning analysis of Les Echets (France) sedimentary sequence: new insights from chemical proxies. *Journal of Quaternary Science* 26, 109–117.
- Laliberte, E., Turner, B.L., Costes, T., Pearce, S.J., Wyrwoll, K.H., Zemunik, G., and Lambers, H., 2012. Experimental assessment of nutrient limitation along a 2-million-year dune chronosequence in the south-western Australia biodiversity hotspot. *Journal of Ecology* 100, 631–642.
- Lascu, I., Banerjee, S.K., Berquo, T.S., 2010. Quantifying the concentration of ferrimagnetic particles in sediments using rock magnetic methods. *Geochemistry Geophysics Geosystems* 11, 22.
- Leys, B., Higuera, P.E., McLauchlan, K.K., and Dunnette, P.V., 2016. Wildfires and geochemical change in a subalpine forest over the past six millennia. *Environmental Research Letters* 11, 125003.

- Likens, G.E., 1985. *An Ecosystem Approach to Aquatic Ecology: Mirror Lake and its Environment*, New York, Springer-Verlag.
- Lopez, P., Navarro, E., Marce, R., Ordoñez, J., Caputo, L., Armengol, J., 2006. Elemental ratios in sediments as indicators of ecological processes in Spanish reservoirs. *Limnetica* 25, 499–512.
- Lusardi, B.A., Jennings, C.E., Harris, K.L., 2011. Provenance of Des Moines lobe till records ice-stream catchment evolution during Laurentide deglaciation. *Boreas* 40, 585–597.
- Mackereth, F.J.H., 1966. Some chemical observations on post-glacial lake sediments. *Philosophical Transactions of the Royal Society B-Biological Sciences* 250, 165–213.
- Maher, L.J., 1982. *The Palynology of Devils Lake, Sauk County, WI: Quaternary History of the Driftless Area*. University of Wisconsin Extension, Geological and Natural History Survey, Madison, Wisconsin.
- Martin-Puertas, C., Tjallingii, R., Bloemsmma, M., and Brauer, A., 2017. Varved sediment responses to early Holocene climate and environmental changes in Lake Meerfelder Maar (Germany) obtained from multivariate analyses of micro X-ray fluorescence core scanning data. *Journal of Quaternary Science* 32, 427–436.
- Maslennikova, A.V., Udachin, V.N., Aminov, P.G., 2016. Lateglacial and Holocene environmental changes in the Southern Urals reflected in palynological, geochemical and diatom records from the Lake Strytkul sediments. *Quaternary International* 420, 65–75.
- Matthews, J.A., 1992. *The ecology of recently deglaciated terrain: A geocological approach to glacier forelands and primary succession*. Cambridge, UK, Cambridge University Press.
- McLauchlan, K.K., Lascu, I., Myrbo, A., Leavitt, P.R., 2013. Variable ecosystem response to climate change during the Holocene in northern Minnesota, USA. *Geological Society of America Bulletin* 125, 445–452.
- Medaris, L.G., Singer, B.S., Dott, R.H., Naymark, A., Johnson, C.M., and Schott, R.C., 2003. Late Paleoproterozoic climate, tectonics, and metamorphism in the southern Lake Superior region and proto-North America: evidence from Baraboo quartzite intervals. *Journal of Geology* 111, 243–257.
- Miao, X., Mason, J.A., Swinehart, J.B., Loope, D.B., Hanson, P.R., Goble, R.J., Liu, X., 2006. A 10,000 year record of dune activity, dust storms, and severe drought in the central Great Plains. *Geology* 35, 119–122.
- Milner, A.M., Fastie, C.L., Chapin, F.S., Engstrom, D.R., Sharman, L.C., 2007. Interactions and linkages among ecosystems during landscape evolution. *Bioscience* 57, 237–247.
- Minyuk, P.S., Borkhodoev, V.Y., Wennrich, V., 2014. Inorganic geochemistry data from Lake El'gygytyn sediments: marine isotope stages 6–11. *Climate of the Past* 10, 467–485.
- Mourier, B., Poulenard, J., Carcaillet, C., and Williamson, D., 2010. Soil evolution and subalpine ecosystem changes in the French Alps inferred from geochemical analysis of lacustrine sediments. *Journal of Paleolimnology* 44, 571–587.
- National Oceanic and Atmospheric Administration (NOAA), 2018. National Weather Forecast (accessed June 03, 2018). <http://www.weather.gov/>.
- Nesbitt, H.W., Young, G.M., McLennan, S.M., Keays, R.R., 1996. Effects of chemical weathering and sorting on the petrogenesis of siliciclastic sediments, with implications for provenance studies. *Journal of Geology* 104, 525–542.
- Norton, S.A., Perry, R.H., Saros, J.E., Jacobson, G.L., Fernandez, I.J., Kopacek, J., Wilson, T.A., SanClements, M.D., 2011. The controls on phosphorus availability in a Boreal lake ecosystem since deglaciation. *Journal of Paleolimnology* 46, 107–122.
- Pawlik, L., Phillips, J. D., and Samonil, P., 2016. Roots, rock, and regolith: Biomechanical and biochemical weathering by trees and its impact on hillslopes—A critical literature review: *Earth-Science Reviews* 159, 142–159.
- Pennington, W.M.T., Haworth, E.Y., Bonny, A.P., Lishman, J.P., 1972. Lake sediments in northern Scotland. *Philosophical Transactions of the Royal Society B-Biological Sciences* 264, 191–294.
- Porder, S., 2014. Coevolution of life and landscapes. *Proceedings of the National Academy of Sciences of the United States of America* 111, 3207–3208.
- Schmidt, R., Kamenik, C., Tessadri, R., Koinig, K.A., 2006. Climatic changes from 12,000 to 4,000 years ago in the Austrian Central Alps tracked by sedimentological and biological proxies of a lake sediment core. *Journal of Paleolimnology* 35, 491–505.
- Sperber, C., Chadwick, O.A., Casciotti, K.L., Peay, K.G., Francis, C.A., Kim, A.E., Vitousek, P.M., 2017. Controls of nitrogen cycling evaluated along a well-characterized climate gradient. *Ecology* 98, 1117–1129.
- United States Department of Agriculture, Natural Resources Conservation Service (USDA NRCS), 2018. Soil Survey | NRCS Soils (accessed June 03, 2018). <http://www.nrcs.usda.gov/wps/portal/nrcs/main/soils/survey/>.
- Vitousek, P.M., and Chadwick, O.A., 2013. Pedogenic thresholds and soil process domains in basalt-derived soils. *Ecosystems* 16, 1379–1395.
- Wardle, D.A., Walker, L.R., Bardgett, R.D., 2004. Ecosystem properties and forest decline in contrasting long-term chronosequences. *Science* 305, 509–513.
- Weltje, G.J., Tjallingii, R., 2008. Calibration of XRF core scanners for quantitative geochemical logging of sediment cores: theory and application. *Earth and Planetary Science Letters* 274, 423–438.
- Williams, J.J., McLauchlan, K.K., Mueller, J.R., Mellicant, E.M., Myrbo, A.E., Lascu, I., 2015. Ecosystem development following deglaciation: a new sedimentary record from Devils Lake, Wisconsin, USA. *Quaternary Science Reviews* 125, 131–143.
- Willis, K.J., Braun, M., Sumegi, P., and Toth, A., 1997. Does soil change cause vegetation change or vice versa? A temporal perspective from Hungary. *Ecology* 78, 740–750.